Metallic Aluminum Activation as Initial Stage for Preparing Alumina Based Catalysts and Supports

M. V. TRENIKHIN[1], V. K. DUPLYAKIN[1], A. I. NIZOVSKIY[2] and A. G. KOZLOV[3]

[1]*Institute of Hydrocarbons Processing, Siberian Branch of the Russian Academy of Sciences, Ul. Neftezavodskaya 54, Omsk 644040 (Russia)*

E-mail: dvk@incat.okno.ru

[2]*Boreskov Institute of Catalysis, Siberian Branch of the Russian Academy of Sciences, Pr. Akademika Lavrentyeva 5, Novosibirsk 630090 (Russia)*

[3]*Rzhanov Institute of Semiconductor Physics, Siberian Branch of the Russian Academy of Sciences, Pr. Mira 55a, Omsk 644077 (Russia)*

(Received September 27, 2005; in revised form December 20, 2005)

Abstract

Initial stage for preparing alumina supported metal catalysts according to a scheme, essentially reducing harmful wastes, is discussed. Preparation method is based on a direct interaction of pretreated metallic aluminum with water. Diffusion phenomena are shown to be the core of aluminum activation by metallic In–Ga alloy. A method for estimating the coefficient of liquid gallium bulk diffusion into the grains of various poly crystal aluminum alloys is suggested.

INTRODUCTION

Industrial manufacturing of many catalysts is known to produce harmful gas exhausts and liquid effluents. A lot of studies focus on the essential reduction of these wastes, or aim at the development of new wasteless catalyst manufacturing technologies. It is well known that most widely used catalysts are alumina-supported systems. One of environmentally harmless ways of alumina catalysts manufacturing is described in [1, 2], which involves the water treatment of preliminarily prepared high purity aluminum alloys with one or several other metals, such as indium, gallium, copper, *etc*. In this case both support and active component form simultaneously, providing ready catalyst uniformity, and allowing other components introduction at the formation stage.

Activated aluminum interaction with water in the presence of other metals yields disperse, thermally stable, porous oxide materials of complex composition and structure based either on alumina modifications or more complex structures [3]. These materials are regarded as promising supports and catalysts for various processes, as well as adsorbents and porous membranes. It is of importance that structure, surface, texture and other physical and chemical properties of such systems differ a lot from the properties of conventionally prepared alumina based oxides either pure or modified.

In the present work we study how aluminum and its industrial alloys interact with a liquid-metallic indium-gallium alloy at ambient temperatures.

EXPERIMENTAL

Aluminum interaction with the liquid-metallic indium-gallium alloy (LMA In–Ga) herein after called “aluminum activation” was performed using In–Ga eutectics, indium content being 24 mass %, and melting temperature being 16 °C [4].

Surface morphology was studied with a raster electronic microscopy (REM) using microscope BS-350 Tesla. The dynamics of LMA In–Ga interaction with chemically pure polycrystal aluminum surface was studied *in situ*. A drop of LMA In–Ga (3 mm^3 in volume) was put on the ethanol treated sample surface for its spreading to be as large as possible. Surface morphology was investigated at the different stages of the sample exposure in the electron microscope chamber at rough vacuum (~1 Pa) or atmospheric pressure, relative moisture being 30–35 %, and temperature being 20 °C.

For the X-ray photoelectron spectroscopy (XPES) studies we took the plates of aluminum alloy AMr3 $5 \times 10 \times 15$ mm in size. Sample surface was investigated using spectrometer ESCA LAB 5 HP (Vacuum generators, UK).

X-ray fluorescence spectroscopy (XFS) was applied to study the bulk aluminum alloys: A-5 (massive ingot, admixture content not higher than 0.5 %, GOST 11069–74); AK5M-2 (bulk ingot, content of alloying elements, mass %: C1.7, Si 4.57, Fe 0.95, Mg 0.58, Mn 0.27, Ti 0.05, Zn 0.7, balance aluminum, GOST 1583–93), deformed industrial alloy AD-1 (bar, 50 mm in diameter, admixtures content not higher than 0.7 %, GOST 4784–74). Grains structure parameters were studied with optical microscopy (microscope MBI-15). Surface morphology was investigated in two perpendicular directions. Average grain size was determined according to GOST 5639–82.

Samples for diffusion studies were shaped as discs (diameter 3 mm, height 5 mm) with a cylinder groove in the disc center (diameter 18 mm, depth 3.5 mm). This shape allowed us to distinguish the processes of bulk and grain limited diffusion. All diffusion studies were done for the indium–gallium–aluminum system at 33–38 °C.

A LMA In–Ga drop approximately 0.5 ml in volume was placed onto the inner surface of the disc groove. XPES was applied for diffusion studies (ARL OPIM'X TERMO ELECTRON, X-ray rhodium anode tube, voltage 25 kV). Lines GaK_α and InL_α were regarded for analysis. X-ray irradiation intensity was measured at the disc side opposite to that containing the LMA In–Ga drop. Diffusion over the disc surface was excluded by its side surface coverage by an organic varnish. For each alloy experiment duration was 10–15 days depending on the sample morphology features. X-ray intensity for both gallium and indium was measured each hour.

RESULTS AND DISCUSSION

REM method, chosen as the most efficient method for studying aluminum surface morphology evolution at its activation, allows one to obtain qualitative data on material conductivity by the character of electron beam reflection. Surface area with a lower conductivity more reflects primary electron beam [5]. This phenomenon shows on the electron photos as bright and light formations (Fig. 1). Therefore, it gave us the opportunity of a more exact interpreting of data related to such a complex manyphase system as Al–In–Ga.

Electron microscopy investigations, registering the changing morphology of activated aluminum surface at the sample exposure in the microscope chamber under rough vacuum, showed no dynamics of LMA In–Ga interaction with aluminum samples. Contact time attained 36 h at 18–20 °C.

In case, when contact occurred at atmospheric pressure, we observed the following typical features of interaction:

1) the increasing roughness of the In–Ga alloy drop surface;

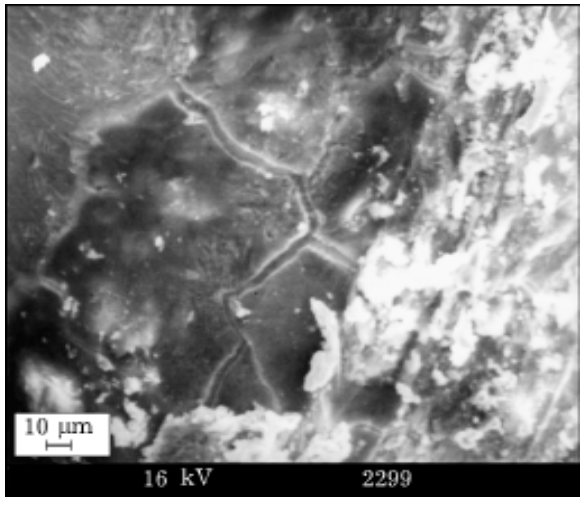

Fig. 1. Polycrystal aluminum surface after a 60 min exposure in the REM chamber at atmospheric pressure.

2) bright areas appearing on the alloy surface illuminating under the electron beam;

3) essentially decreasing alloy volume;

4) both darker and brighter areas appearing on aluminum surface near the LMA In–Ga drop in comparison to the starting one.

The first signs on above mentioned morphology changes appeared in 20–30 min after contact started at 18–20 °C, and intensified in time. After 20–25 h we visually observed the "roughening" of aluminum surface.

A detailed analysis of electron microscopy images reveals a definite character of the objects behavior. Thus, as atmospheric exposure increases, the portion of bright parts on aluminum and LMA drop surface also increases. The zone of illuminating aluminum surface is always surrounded by the dark zone. As we have already noted, illuminating zones appear, when the conductivity of some surface areas decreases. There are also some interesting features of the zones location. There is no continuous coverage near the LMA drop. Spottiness often coincides by its spread with the area of aluminum grains in the initial sample. Narrow illuminating zones appear along the grains perimeter, while interfaces show a rather good conductivity, *i.e.* well absorb electrons emitted by the microscope cathode (Fig. 2). Therefore, alloy In–Ga forms a film along the grain boundaries, providing the expansion of grain boundaries at sample activation, as is registered on the electron microscopy photos.

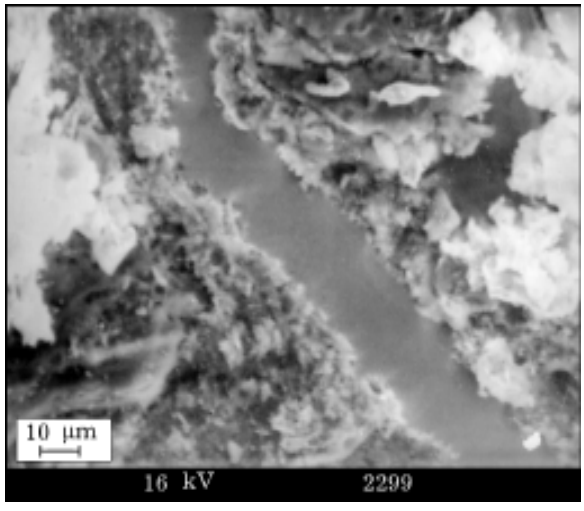

Fig. 2. Surface area showing the product of LMA In–Ga interaction with aluminum. Photo diagonal demonstrates the LMA In–Ga film, formed along the grain boundary.

The further studies of aluminum activation process were arranged as follows. In order to distinguish the effects related to water vapor influence from the other effects at atmospheric exposure, we put some aluminum samples after activation into the silica gel containing vessel, and other samples into the vessel, containing water vapors at $P/P_s = 1$. In the first case, when samples were kept in the dry atmosphere, activity in water decomposition essentially depended on exposure time t_w from the moment of the LMA In–Ga removal from the sample surface. We have noticed a threshold exposure time, $t_w \sim 10$ h, after that we saw no significant change in aluminum dissolving efficiency. Many time repeated experiments (samples were activated by the full dipping into the LMA In–Ga) at 18 and 35 °C demonstrate a pronounced passivation (inhibition) by water vapours at $P/P_s = 1$, which was independent of t_w.

We applied XPES to reveal the role of water vapours. For all samples initial XPES spectra show mostly surface oxides of In, Ga and Al (Fig. 3). We used an Ar^+ etching to characterize components distribution in the subsurface layers.

In the case of activated samples, then exposed to the dry atmosphere, spectrum metal constituent at Ga2*p*, In3*d* appears after 5 min of etching. Earlier etching estimates at the given etching parameters (~0.5 nm/min) confirm the layer thickness to be ~2.5 nm. As etching continues, spectrum oxide constituent decreases, and attains ~10 % at $t_{etch} = 100$ min.

Therefore, according to the XPES data, the main portion of subsurface aluminum is in the oxidized state, which is in a good agreement with the REM results. Indium and gallium are in metallic state (see Fig. 2), while zones between the grains have no charge supply, and look like smooth enough "river" like formations.

In a thick layer (~50 nm) indium and gallium concentrations grow, and depend on t_w. Note, that Al^{ox} phase, present in large quantity, confirms the fact that oxygen amount is not decreasing on etching.

The XPES spectra of samples exposed to water vapors demonstrate quite a different picture. They do not reveal intensive enough peaks corresponding to metallic state, and show

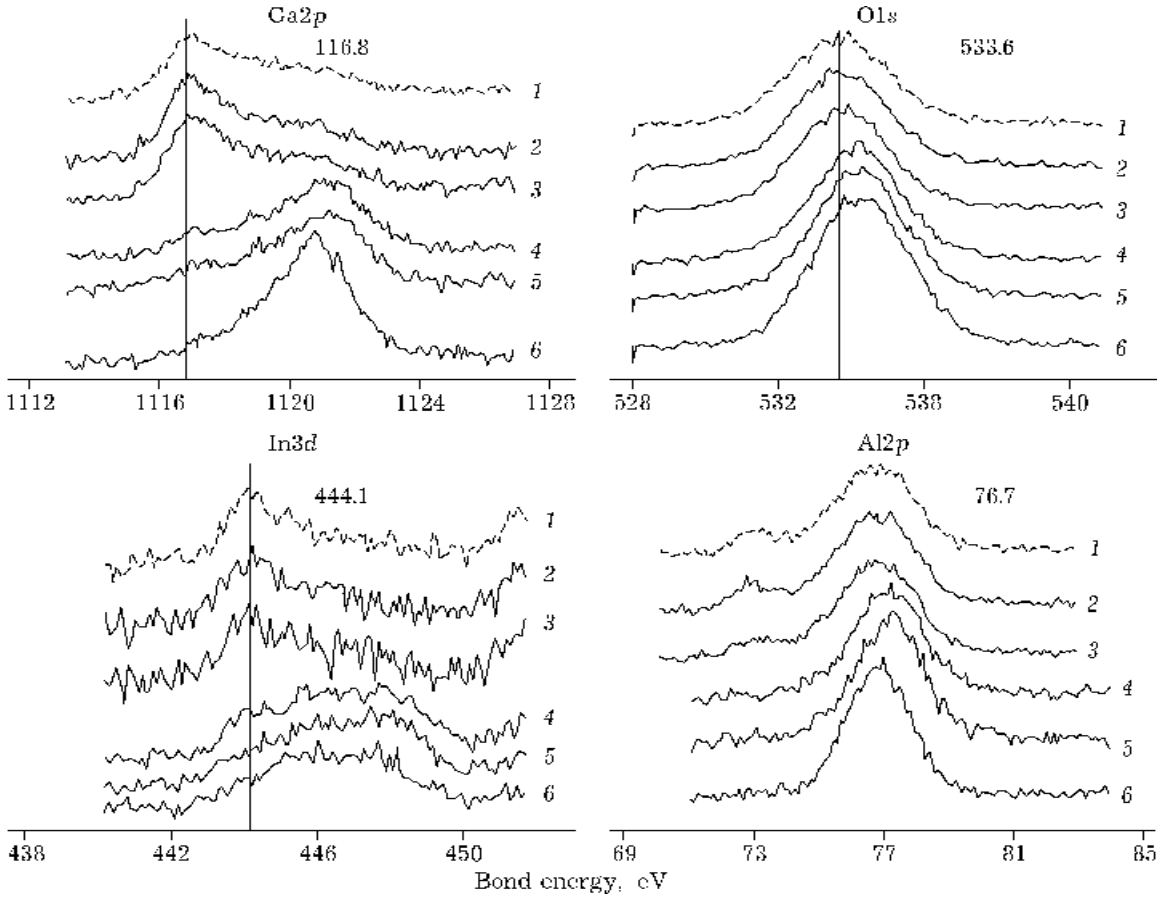

Fig. 3. XPES spectra of aluminum surface after ion etching in spectrometer chamber. Etching time, min: 100 (*1*), 80 (*2*), 45 (*3*), 10 (*4*) and 5 (*5*), no etching (*6*). The time of sample storage in dry atmosphere is 3 h.

the following tendency: $In^{met}/In^{ox} > Ga^{met}/Ga^{ox}$. The total concentration of alloy components in the subsurface layer is considerably lower than in the case of samples exposure to dry atmosphere.

Therefore, water may block the process of LMA penetration into aluminum and oxidize its components.

The LMA component re-dispersion in the aluminum grains is most likely responsible for the increase of gallium concentration on etching (Fig. 4). According to the XPES data this effect is well known for the supported catalysts. If we consider two catalysts with the same mass portion of the supported component, the more dispersed sample is visually characterized by the higher concentration.

We have also studied how the LMA In–Ga components penetrate along the grain boundaries, as well as gallium bulk diffusion into aluminum grain.

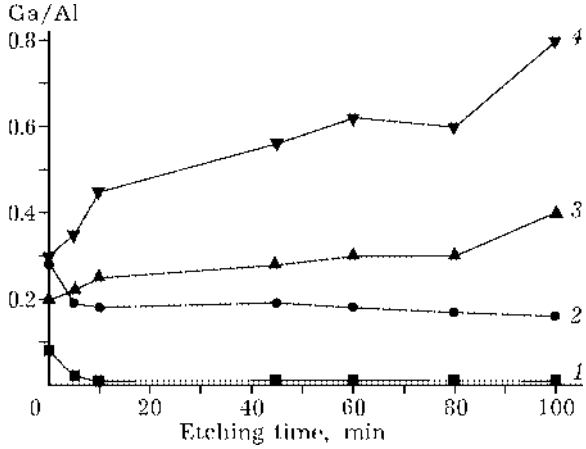

Fig. 4. Gallium and aluminum concentration *versus* the time of aluminum surface etching by argon ions: *1* – sample immediately after activation; etching time, h: 3 (*2*), 11 (*3*) and 24 (*4*).

Optical microscopy shows that in alloys A-5 and AK5M-2 grain shape is averagely the same longwise and crosswise the ingot. In alloy AD-1 we observe specific texture along the bar. The

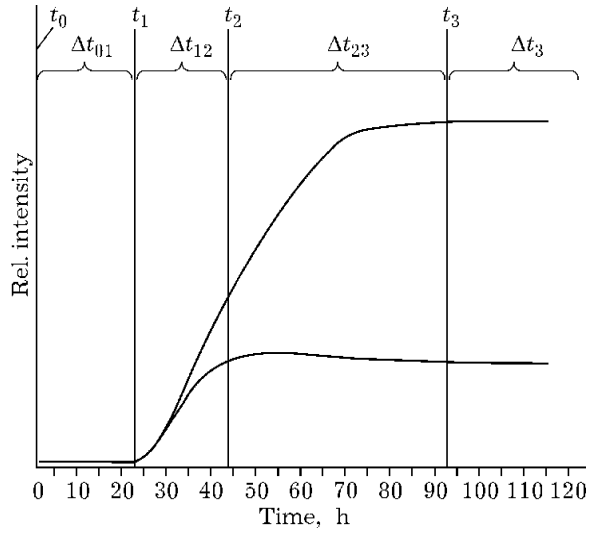

Fig. 5. GaK_α and InL_α intensity *versus* time for alloy AD-1.

average diameters of grains in various alloys are as follows: A-5 – 85 μm, AK5M-2 – 60 μm, AD-1 (crosswise) – 50 μm.

According the XFS data GaK_α and InL_α intensities as time functions are similar for all aluminum alloys (see Fig. 5 as an example for alloy AD-1). The combined plot of intensities reveals four typical time intervals: Δt_{01}, Δt_{12}, Δt_{23}, Δt_{38}. In interval Δt_{01} there is no GaK_α and InL_α irradiation on the opposite side of the sample. This interval begins with the experiment start at t_0, and finishes at t_1, when GaK_α and InL_α X-ray irradiation appears on the opposite side of the disc. In time interval Δt_{12} gallium and indium irradiation intensities grow simultaneously. Interval finishes (t_2), when InL_α intensity becomes constant, while GaK_α continues to grow. Interval Δt_{23} is a period, when only GaK_α intensity is growing, and interval finishes (t_3), when gallium irradiation intensity stops growing. In interval Δt_{38} both gallium and indium X-ray irradiation intensities are constant. This interval finishes with the experiment. In our case we observed constant irradiation intensities for 7 days.

One may explain the XFS data considering peculiarities of indium and gallium diffusion in aluminum. According to the Hume–Rothery rule [6] metals dissolving in the solid state is limited, if the difference between atomic radii of alloy forming elements does not exceed 14–15 %. According to various references [7, 8] average atomic radii for aluminum, gallium and indium are 0.137, 0.130 and 0.164 nm, respectively. Essential difference between atomic radii of In and Al (more than 15 %) may cause poor In dissolving in aluminum. According to the reference data [9] this value is less than 0.01 mass %. On the contrary, similar atomic radii of gallium and aluminum conditions good Ga dissolving in aluminum, which attains 21 mass % [10]. Therefore, it is assumed that at ambient temperatures gallium diffuses into aluminum grains, thus producing a solid solution with aluminum substitution for gallium according to the Al–Ga state diagram. Another peculiarity is that at first gallium diffuses into poly crystal aluminum and its alloys along the grain boundaries [11, 12]. Since grain boundary diffusion coefficient considerably exceeds the bulk one [13], at initial stage gallium bulk diffusion in aluminum grains is insignificant for aluminum saturation. If the characteristic size of solid sample is small, then grain boundary diffusion is even more important.

Regarding all above-mentioned ideas we may suggest the following mechanism of processes occurring at the LMA In–Ga contact with aluminum based alloys, allowing us to explain the XFS data (see Fig. 5). At first LMA In–Ga penetrates into aluminum alloy along the grain boundaries. At moment t_1 penetration front gets to the opposite side of the sample. The fact, that at the same moment In and Ga irradiation intensities start growing, proves that LMA In–Ga penetrates altogether, but not by its individual elements. In Δt_{12} aluminum alloy is saturated by LMA In–Ga due to the LMA penetration along the grain boundaries. This period finishes at t_2, when InL_α irradiation intensity stops growing. Taking into account poor In dissolving in aluminum, we may assume that In accumulates mostly along the grain boundaries. Its concentration attains saturation owing to the LMA In–Ga diffusion over the grain boundaries. Then in Δt_{23} aluminum alloy is saturated only by Ga exclusively due to the bulk Ga diffusion inside aluminum grains. At t_3 diffusion saturation stops, and concentration of the LMA In–Ga components in aluminum alloy attains its threshold value.

Therefore, analysing the XFS plots (see Fig. 5) we may assume that time moment, when InL_α intensity stops growing (t_2), is a qualitative

sign that LMA In–Ga penetration into aluminum alloy is completed. In this case time interval Δt_{23} characterizes bulk gallium diffusion into aluminum grains. It allows us to estimate its bulk diffusion coefficient choosing appropriate mathematical model.

In our experiments the quantity of LMA In–Ga exceeded that of aluminum alloys. Therefore, it is reasonable to use diffusion, model with a surface source of infinite capacity. In alloys A-5 and AK5M-2 grains shape is the same in all directions. In this case we may use the model of diffusion saturation in a sphere with admixture source on the sphere surface. According to this model diffusion saturation may be written as:

$$C(r,t) = 2C_0 \sum_{n=1}^{\infty} \frac{-(-1)^n R}{n\pi r} \sin\left(\frac{n\pi r}{R}\right) \times \left[1 - \exp\left(-\frac{n^2\pi^2 D_{\text{bulk}} t}{R^2}\right)\right] \quad (1)$$

here $C(r,t)$ is gallium concentration in the spherical particle, C_0 is gallium concentration on the spherical particles surface, r is the distance from the spherical particle center, t is diffusion time, R is the radius of spherical particle, D_{bulk} is the coefficient of gallium bulk diffusion [14].

For textured alloy AD-1 diffusion saturation in a cylinder with admixture source on the cylinder surface seems to be appropriate. In this case diffusion saturation follows equation:

$$C(r,t) = 2C_0 \sum_{n=1}^{\infty} \frac{1}{\mu_n J_1(\mu_n)} J_0\left(\frac{\mu_n r}{R}\right) \times \left[1 - \exp\left(-\frac{\mu_n^2 D_{\text{bulk}} t}{R^2}\right)\right] \quad (2)$$

here J_0, J_1 are the zero and first order Bessel functions, respectively; μ_n are solution roots for equation $J_0(\mu)$. Other signs correspond to those from equation (1), but refer to a cylinder particle.

In both models equation (3) was taken as criterion for diffusion saturation:

$$C(r,t)\big|_{r=0} = 0.9C_0 \quad (3)$$

With this condition solving equations (1) and (2) we determine ratio $D_{\text{bulk}}t/R^2$ entering the exponent: 0.305 and 0.43 for the spherical and cylinder particle, respectively. Using these various and taking diffusion time as Δt_{23}, we may obtain gallium bulk diffusion coefficient for the spherical particle:

$D_{\text{bulk}} = 0.305R^2/\Delta t_{23}$

and for the cylinder particle:

$D_{\text{bulk}} = 0.43R^2/\Delta t_{23}$

The calculated coefficients D_{bulk} for gallium bulk diffusion in aluminum alloys are, cm^2/s: A-5 – $1.1\ 10^{-10}$, AK5M-2 – $1.5\ 10^{-11}$, AD-1 – $6.1\ 10^{-11}$. The spread of diffusion coefficient values may be explained by, first, different defectiveness of aluminum grains in different alloys, second, by the presence of different alloying elements, affecting gallium diffusion. Let us note that reference data also differ a lot [15–18], most likely due to the different structure and composition of the studied samples. Thus, according to [15] gallium diffusion coefficient in monocrystal alumina in a temperature range of 400–650 °C is $1.8\ 10^{-10}$–$5.6\ 10^{-8}$ cm^2/s. Diffusion coefficient, calculated according to the X-ray spectra microanalysis [17] at 250 °C, is $2\ 10^{-10}$ cm^2/s. Values extrapolation to ambient temperature shows that D_{bulk} we calculated is higher than those reported in [15, 17]. This difference may be explained by essential defectiveness of aluminum grains in the alloys. In particular, at a large number of dislocations in alloys gallium diffusion transfer over dislocations dominates over gallium transfer by the point defects, the latter being more influential in monocrystal materials.

These results may be considered as a conceptual base for the development of alumina and its alloys activation application at the starting stage of environmentally harmless technologies to produce:

– high purity hydrogen for fuel cells;

– high purity alumina of various phase composition and texture, regulated by the conditions of alumina activation by water;

– new nanostructure materials, *e.g.* spinels, when dopes with high specific surface (150 m^2/g and larger) are introduced into water solution at temperatures above 1000 °C;

– catalytic systems presented by supported highly disperse metals or metal oxides, forming when activated alumina interacts with water solutions containing active component precursors.

The suggested method enables to obtain many component catalysts by components mixing at atomic scale in the course of activated alumina oxidation by water, while catalytically active precursor (*e.g.*, platinum, palladium or nickel compounds) reacts with evolving hydrogen. Thus with high probability one may produce various structures homogeneous on microscale, when a matrix (aluminum hydroxide) intensively interacts with a catalytically active component, providing significant modification of adsorption and catalytic properties of ready products.

Further publications will report on the field development.

CONCLUSIONS

1. According to the REM data LMA In–Ga contact with aluminum surface in rough vacuum has no effect at all, but at atmospheric pressure and relative moister 30–35 % it yields new dielectric products – aluminum hydroxides. XFES method shows that in the presence of water vapour there is no aluminum activation, and aluminum surface is blocked by the oxides of aluminum, indium and gallium. Therefore, for the most intensive aluminum activation it is necessary to remove water completely from the sample environment.

2. XFS data were important for determining the characteristic time intervals of aluminum alloys activation by the In–Ga alloy with regard to the alloy type and geometric shape.

3. The obtained results seem to be promising for the application of aluminum activation by the In–Ga alloys at catalysts manufacturing. They also open ways for various catalytic applications: synthetic fuels production, combustion of toxic and flame gases, environmental monitoring of harmful gases.

REFERENCES

1 R. G. Sarmurzina, V. I. Yakerson, D. V. Sokol'skiy *et al.*, *Dokl. AN SSSR*, 283, 2 (1985) 427.
2 L. A. Kozin, R. G. Sarmurzina, *Zh. Prikl. Khim.*, 10 (1981) 2176.
3 V. I. Yakerson, Zh. L. Dykh, A. N. Subbotin *et al.*, *Kinetika i Kataliz*, 39, 1 (1998) 108.
4 S. P. Yatsenko, V. I. Kononenko, V. N. Danilin *et al.*, Svoystva galliya v vodnykh rastvorakh i splavakh, Sverdlovsk, 1965.
5 J. Goldstein, D. Newbery and P. Echlin, Scanning Electron Microscopy and X-ray Microanalysis, Plenum, New York, 1981.
6 V. Yum-Rozeri, Vvedeniye v fizicheskoye metallovedeniye, Metallurgiya, Moscow, 1965.
7 Ch. S. Barret, T. B. Massal'skiy, Struktura metallov, Moscow, 1984.
8 A. T. Pilipenko, Kratkiy khimicheskiy spravochnik, Nauk. Dumka, Kiev, 1987.
9 S. P. Yatsenko, Indiy: svoystva i primeneniye, Nauka, Moscow, 1987.
10 R. V. Ivanova, Khimiya i tekhnologiya galliya, Metallurgiya, Moscow, 1973.
11 L. N. Larikov, E. A. Maksimenko, V. I. Franchuk, *Metallofizika*, 12, 2 (1990) 115.
12 L. N. Larikov, V. I. Franchuk, E. A. Maksimenko, *Ibid.*, 13, 10 (1991) 3.
13 I. Kaur, V. Grust, Diffuziya po granitsam zeren, Mashinostroyeniye, Moscow, 1991.
14 Ya. E. Geguzin, Diffuzionnaya zona, Nauka, Moscow, 1979.
15 N. L. Peterson, S. J. Rothman, *Phys. Rev. B*, 1 (1970) 3264.
16 R. C. Hugo, R. G. Hoagland, *Acta Mater.*, 48 (2000) 1949.
17 L. N. Larikov, E. A. Maksimenko, V. I. Franchuk, *Metallofizika*, 15,3 (1993) 44.
18 B. I. Zilbergreit, S. P. Yatsenko, *Zh. Prikl. Khim.*, 44 (1970) 1303.